J3.4

PREDICTABILITY IN PAST AND FUTURE CLIMATE CONDITIONS: A PRELIMINARY ANALYSIS BY NEURAL NETWORKS USING UNFORCED AND FORCED LORENZ SYSTEMS AS TOY MODELS

Antonello Pasini *

CNR, Institute of Atmospheric Pollution, Rome, Italy

1. INTRODUCTION

It is well known that the climate system can be considered as the prototype of a complex system, as it is composed by many subsystems and endowed with a lot of cause-effect circular chains.

At present, Global Climate Models (GCMs) represent the main tools for grasping this complexity in a fully dynamical way. In particular, GCMs showed good results in their applications to reconstruction and attribution of recent climate change and they supply us with projections of future climate scenarios, too. However, despite of these positive features, their "building strategy" (conceptually described in Pasini 2005) suffers from some drawbacks, e.g. the need to fine-tune some coupling parameters: this leads to a non-univocal reconstruction of the real system in the simulated model (an extensive discussion about this problem can be found in Pasini 2007).

The recognition of the great complexity of GCMs and their dynamical behavior, together with the awareness of their drawbacks, led to adopt alternative strategies for catching the complexity of the climate system in a more direct and simple way. An example of these strategies can be found in Pasini et al. (2006), where the application of a neural network (NN) non-dynamical model to the problem of attribution and reconstruction of the recent global and regional warming is described. Another well-founded strategy is the adoption of a "dynamical perspective" for the study of climate and the investigation of low-dimensional dynamical systems' behavior in cases when this can resemble the dynamics of the real system: see Palmer (1993, 1999) for this approach.

With reference to this latter strategy, it is worthwhile to stress that the classical Lorenz model (Lorenz 1963) mimics some features of the climate system (and its atmospheric subsystem), such as their chaotic behavior and the existence of preferred states or "regimes". Furthermore, distinct regions on the Lorenz attractor show different predictabilities, exactly as distinct types of weather situations are endowed with different predictability horizons. Finally, changes in the frequency of occurrence of regimes can be observed both in the real system and in the toy Lorenz model, when external forcings increase.

* *Corresponding author address:* Antonello Pasini, CNR, Institute of Atmospheric Pollution, via Salaria Km 29.300, I-00016 Monterotondo Stazione (Rome), Italy; e-mail: pasini@iia.cnr.it

In this framework, one can be induced to use the Lorenz system as a toy model for studying the course of predictability in past and future climate conditions. In particular, in this paper the ability of a NN model to recognize regions of distinct predictability on the Lorenz attractor is shown, even vs. dynamical estimations. Moreover, once added an external forcing to the Lorenz system (as a toy simulation of increase in anthropogenic forcings to the climate system), changes of predictability in this new scenario are found by both dynamical quantities and NN modeling. Finally, an attempt at an "operational" NN estimation of predictability on the unforced and forced attractors is investigated, too.

In what follows I will briefly describe the NN tool developed by me and coworkers during the last years (section 2) and the dynamical properties of unforced and forced Lorenz models (section 3). Then, NN modeling will be applied to a forecast activity on the Lorenz attractors and consequences for predictability estimations will be discussed (section 4). In section 5 an attempt at achieving an operational estimation of predictability in the unforced and forced situations will be performed. Finally, brief conclusions will be drawn and prospects of further study will be envisaged in the last section.

2. THE NN TOOL

A NN tool for both diagnostic characterization and forecast in complex systems has been developed some years ago (Pasini and Potestà 1995). Since that date it has been applied to diagnostic and prognostic problems in the boundary layer (Pasini and Potestà 1995, Pasini et al. 2001, 2003a,b, Pasini and Ameli 2003) and recently, as cited above, also to the analysis of climatic data (Pasini et al. 2006).

As far as the kernel of this NN tool is concerned, it has been extensively described elsewhere (see, for instance, Pasini et al. 2003a). Here, it is sufficient to note that the NNs adopted are feedforward and characterized by a backpropagation training endowed with gradient descent and momentum terms in the rules for weights updating. Furthermore, an early stopping method is also available.

Together with these quite standard features (see Hertz et al. (1991) and Bishop (1995) for two reviews on these topics), this tool provides us many training facilities, useful for handling historical data from complex systems. As far as the topology of these NNs is concerned, it consists of one input layer, one hidden layer and one output layer.

Finally, it is worthwhile to stress that in what follows the attention will be paid more on the possibility of achieving certain results by NN modeling than on the rate of performance obtained by the specific model adopted. As we will see, increase in performance can be envisaged by use of different input variables and/or different NN models.

3. SOME DYNAMICAL PROPERTIES OF UNFORCED AND FORCED LORENZ MODELS

As cited above, from a physical point of view the Lorenz model mimics some characteristic features of both atmosphere and climate. On the other hand, it has also a general relevance as far as its mathematical structure is concerned: it can be considered as the prototype of a large class of models of meteo-climatic importance (see Pasini and Pelino (2000) for the recognition of this class and the development of an extended formalism).

Thus, here the Lorenz model (in its unforced and forced versions) will be adopted without delay for investigation: in this section, its dynamical properties will be analyzed.

The classical Lorenz system (Lorenz 1963) reads as follows:

$$\begin{cases} \dfrac{dx}{dt} = \sigma(y-x) \\ \dfrac{dy}{dt} = rx - y - xz \\ \dfrac{dz}{dt} = xy - bz \end{cases} . \qquad (1)$$

Here the choice of the parameters is the same as in Lorenz (1963), that is σ = 10, b = 8/3, r = 28: this leads to a chaotic behavior.

The numerical integration of this system is performed through a 4th-order Runge-Kutta scheme with time step Δt = 0.01. After an initial transient period, the trajectories lie on a strange attractor endowed with fractal dimension (see Figure 1 for a picture of its projection onto the *x-y* plane). The states of the system oscillate chaotically around two symmetrical unstable fixed points and the left and the right “wings” of the attractor (which one can interpret as the regimes of the Lorenz model) are equally “visited” (in frequency) by the states themselves.

This classical Lorenz model has been recently revisited in connection with studies about changes in atmospheric regimes induced by external forcings. In particular, Palmer and coworkers (Palmer 1999, Corti et al. 1999) showed that the observed climate change of the last decades "can be interpreted in terms of changes in the frequency of occurrence of natural atmospheric circulation regimes" (Corti et al. 1999). In this framework, the Lorenz system (with its wings-regimes) represents a toy model in which we can recover a similar behavior, if it is forced by a weak external forcing. From this viewpoint that forcing can be interpreted as the analogue of the increase of anthropogenic forcings in the real climate system. A further research showed that a weak forcing added to the original unforced Lorenz model can lead to a relevant increase in the frequency of occurrence of extremely persistent events (Khatiwala et al. 2001).

Following the formalism by Palmer (1999), a forced Lorenz system reads as follows:

$$\begin{cases} \dfrac{dx}{dt} = \sigma(y-x) + f_0 \cos\theta \\ \dfrac{dy}{dt} = rx - y - xz + f_0 \sin\theta \\ \dfrac{dz}{dt} = xy - bz \end{cases} . \qquad (2)$$

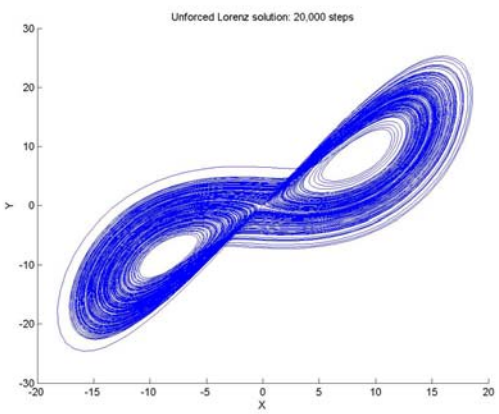

Figure 1. Projection of the classical Lorenz attractor onto the *x-y* plane.

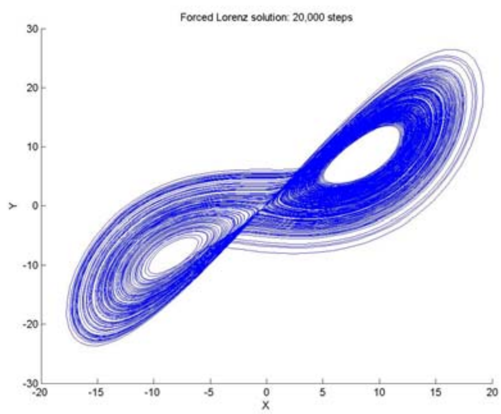

Figure 2. Projection of the forced Lorenz attractor with f_0 = 5 and θ = 90° onto the *x-y* plane: right wing is visited more frequently by the states of the system.

Of course, when f_0 = 0 we recover the classical unforced Lorenz system (1). Furthermore, Mittal et al. (2005) showed that putting a non-vanishing forcing also in the third equation is equivalent to retain the forcings in the first two equations and to shift the parameter *r*. Thus, we consider the form (2) of the forced Lorenz system as a quite general one. In what follows I explore the case θ = 90°.

As one can see in Figure 2, in this forced case the shape of the attractor does not change substantially, but the states of the system "visit" the two wings-regimes in a different manner: this forcing leads to increase the frequency of occurrence of the regime which lies in the positive *x-y* quadrant. A rigorous investigation of this phenomenon can be performed if the probability density function of the states associated with the two wings-regimes is calculated, as in Palmer (1999). Here, I quantify this effect by calculating the mean values $\bar{x}$, $\bar{y}$ and $\bar{z}$ (shown in Table 1 for several values of f_0): one can appreciate a net bias towards the positive *x-y* quadrant which presents a quasi-linear proportionality to the strength of the forcing.

Apart from the bias just discussed, other dynamical properties of the Lorenz attractor reveal litlle changes when forcing increases, at least till f_0 = 5: this value is considered a limit beyond which the model behavior changes qualitatively (see, for instance, Annan 2005), finally reaching the situation of a stable fixed point as attractor. In Table 1 the values of the positive Lyapunov exponent (PLE) and of the fractal dimension of the attractor (DIM) are shown (refer to Wolf et al. (1985) and Briggs (1990) for methods of calculation). As well known, their values represent two "measures" of chaos. Note that the differences between the unforced values and the forced ones of PLE and DIM are very little when f_0 = 2.5 is considered, while they are quite significant when the forcing is doubled.

Var.	$F_0 = 0$	$f_0 = 2.5$	$f_0 = 5$	$f_0 > 10$
$\bar{x}$	-0.0476	1.1838	2.7596	f. p.
$\bar{y}$	-0.0473	1.1845	2.7608	f. p.
$\bar{z}$	23.526	23.643	24.029	f. p.
PLE	0.905	0.880	0.759	< 0
DIM	2.062	2.060	2.053	0
$\bar{g}$	9.06 x 10^{-3}	8.90 x 10^{-3}	7.56 x 10^{-3}	< 0

Table 1. Dynamical variables for the classical unforced Lorenz system (f_0 = 0) and for several forced Lorenz systems with θ = 90° (f. p. means that when f_0 > 10 the attractor is a fixed point whose coordinates depend on the intensity of f_0).

After this brief dynamical analysis of unforced and forced attractors, let's come to the topic of predictability. The local predictability on the unforced Lorenz attractor has been extensively studied in Evans et al. (2004) by means of the so called bred-vector growth, i.e. the rate of divergence of trajectories starting from very close points on the attractor itself.

A bred vector is a vector $\delta\vec{v}$ which simply represents the 3D-Euclidean distance between two states (points) on the Lorenz attractor after a certain number (*n*) of time steps in two model runs, if the second run is originated from a slight perturbation ($\delta\vec{v}_0$) in the initial conditions. We define the bred-growth rate *g* as:

$$g = \frac{1}{n} ln\left(\frac{|\delta\vec{v}|}{|\delta\vec{v}_0|}\right). \quad (3)$$

As shown in Evans et al. (2004), *g* can be used to identify regions of distinct predictability on the unforced Lorenz attractor. Furthermore, these authors were able to find prediction rules for regime changes and persistence in a new regime.

Notably, these prediction rules will be reconsidered and improved by Yadav et al. (2005), who extended their investigation to forced Lorenz models, too. However, if we exclude this peculiar discovery, no attempt at estimating global or local predictability on forced Lorenz models has been performed, at my knowledge.

Here, by adopting the method by Evans et al. (2004), after having fixed *n* = 8, a total of 60,000 bred-growth rates have been calculated, 20,000 related to points of the unforced attractor and the others related to states of two forced attractors with f_0 = 2.5 and f_0 = 5, respectively. The results for the mean values of *g* are presented in Table 1, while in Figures 3 and 4 two plots of growth-rate classes on the unforced and a forced attractor are shown. In Table 2 the notation adopted for the specific division into predictability classes is explained.

Even if from a quick look at Figures 3 and 4 it is plain that regions of distinct predictability exist on the attractors, these two pictures are quite similar and we are not able to distinguish clear changes in the local predictability distributions. However, an analysis of the mean values of *g* ($\bar{g}$) in Table 1 shows that a sensible (nonlinear) decrease in the bred-growth rate happens when the forcing achieves f_0 = 5. Some more piece of information is given in Table 3, where the number of states associated with a certain class of *g* is shown: clearly, one is able to appreciate the consistent increase in the blue class and the even more significant decrease in the red class when passing from the unforced situation to the forced one with f_0 = 5.

Class	Bred-growth rate
Blue	$g < 0$
Green	$0 \leq g < 0.04$
Yellow	$0.04 \leq g < 0.064$
Red	$g \geq 0.064$

Table 2. The predictability classes considered in this study.

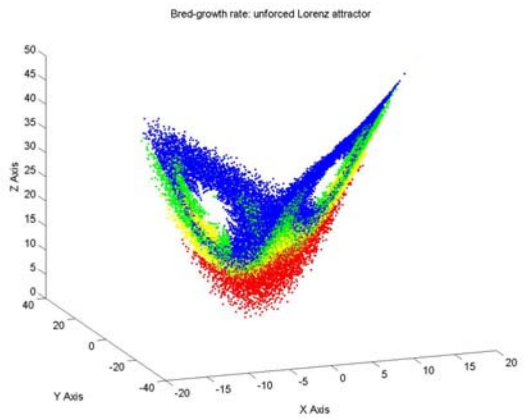

Figure 3. Regions of distinct local predictabilities on the unforced Lorenz attractor.

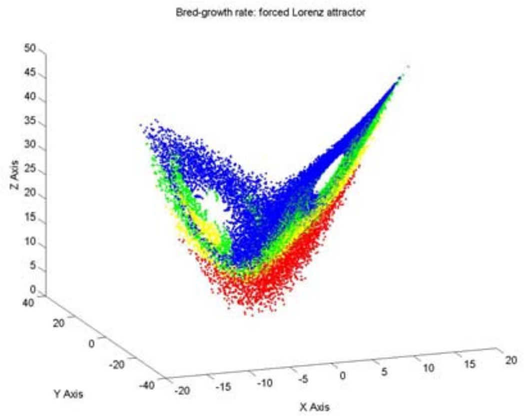

Figure 3. Regions of distinct local predictabilities on a forced Lorenz attractor with f_0 = 5 and θ = 90°.

Class	$f_0 = 0$	$f_0 = 2.5$	$f_0 = 5$
Blue	10185	10270 (+0.8%)	10535 (+3.4%)
Green	4469	4475 (+0.1%)	4488 (+0.4%)
Yellow	2569	2526 (-1.6%)	2601 (+1.3%)
Red	2777	2729 (-1.8%)	2376 (-14.4%)

Table 3. Number of states belonging to each class of predictability on the unforced Lorenz attractor and on two forced ones.

As a consequence of this brief dynamical analysis, in what follows I will limit to compare results between the unforced situation and the case f_0 = 5: this value of the external forcing is enough for obtaining consistent dynamical differences but does not change the general (chaotic) behavior of the model. This will allow me to avoid problems about results' interpretation encountered in a previous paper (Pasini and Pelino 2005).

4. CHANGES IN PREDICTABILITY RECOGNIZED BY NN FORECASTING

Forecasting future states of the Lorenz system by NNs is not a new idea. Nevertheless, past attempts essentially dealt with the prediction of the time series for a single variable of the Lorenz system (usually the *x* variable), with the aim of reconstructing its complete dynamics under the conditions prescribed by the Takens theorem (Takens 1981): see, for instance, de Oliveira et al. (2000) and Boudjema and Cazelles (2001), and references therein. This permits to mimic the reconstruction of an unknown dynamics by observational data in a complex system.

A notable paper, which is correlated enough with the discussion at the previous section about regime changes, is that by Roebber and Tsonis (2005), where the authors used NNs as a method to improve the prediction of flow transitions in the cases of two simple mathematical systems.

Here, my aim is different. I would like to answer the following questions: “Is NN forecasting performance related to local predictability?”; then: “Can one appreciate changes in predictability in forced situations by means of NN forecasting performance?”; and finally: “Can NN modeling supply us with an operational estimation of the predictability on the Lorenz attractors?”.

In doing so, I consider the full dynamics of the unforced and forced Lorenz systems (with 3 inputs, one for each variable, in this attempt). Here I do not discuss how to choose the optimal topology for networks. It is worthwhile to stress that 15 neurons are included in a single hidden layer: this number is sufficient to obtain a good representation of the underlying function but not so big to determine some kind of overfitting.

Now, for each class of bred-growth rate, the NN model is trained to make a single-step forecast from t_0 to $t_0 + n$ (here, of course, n = 8 is chosen, as in the bred-growth calculations). Attempts at performing 8 forecast steps (to achieve the same final forecast horizon) result in very poor performance, as already noted in other studies (Pasini and Ameli 2003) and as known from theoretical considerations (Atiya et al. 1999). The total sets of Lorenz simulated data (20,000 input-target patterns for each case) are divided into a training set (80% of data) and a validation/test set (20%). The networks are endowed with 3 outputs (the 3-dimensional position after 8 time steps of integration). Furthermore, here the 3D-Euclidean distance between output and target points is considered as a measure of forecasting performance: of course, lower is this distance better is the performance of the NN model.

As shown in Table 4, the mean errors of the NN model (expressed in terms of the mean distance between output and target points) clearly depend on the bred-growth classes and exhibit the best performance on the blue region of the attractor and the worst one on the red points. Performance on green and yellow classes presents intermediate values and, even if it is impossible to distinguish between them because each value falls inside the error bar associated to the other one, however these are well separated from the performance values of the other two classes (blue and red). In this Table, together with the mean distance between output and target points, error bars coming from ensemble runs of the model are shown. This is a way for permitting the networks to widely explore the landscape of the cost function and for assessing uncertainties in the results: these error bars represent ± 2 standard deviations.

Class	$f_0 = 0$	$f_0 = 5$
Blue	5.66 ± 0.15	5.24 ± 0.23
Green	6.58 ± 0.25	6.14 ± 0.20
Yellow	6.62 ± 0.24	6.11 ± 0.30
Red	8.36 ± 0.41	8.30 ± 0.45

Table 4. Performance of NN forecasts on the test sets in terms of mean distance between output and target points.

When the forced system is considered, analogously to the decrease of the mean value of *g* in Table 1, also the total mean forecast error of the NN model decreases. This is an expected result, because now there is a net shift of less predictable points to more predictable ones (see Table 3), with a more frequent permanence of the system's state in regions of high predictability. Furthermore, the results on the blue region shows a statistical significant improvement in performance in this specific class and also the improvements in green and yellow class are close to a full statistical significance: this could suggest that changes in predictability, locally on the attractor, can be important, even if this hypothesis is not verifiable in this context.

In any case, the goodness of a NN forecast is related to the specific class of predictability. Moreover, we can appreciate a net increase in both dynamical predictability and NN performance in a forced situation.

A closer look at these results, in terms of the distributions of NN forecast errors for each class, permits to reveal that unimodal distributions (for blue and green classes) tend to split to quasi-bimodal distributions for yellow and red classes. In Figures 5 and 6 these distributions are shown for the blue and the yellow class, respectively, in the unforced case. Similar results hold for NN modeling on the forced systems. This fact implies a sensitivity of forecast performance to regions where a change of regime is possible and two close trajectories could evolve to opposite wings on the attractor. For instance, if one refers to Figures 3 and 4, it is very clear that the trajectories which end onto red points come from the middle of the attractor where they undergo a "bifurcation" towards the left or the right wing of the attractor itself.

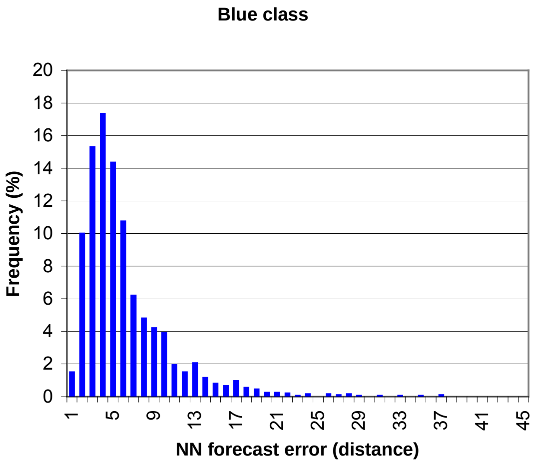

Figure 5. Error distribution in NN forecasts for the blue class on the unforced attractor.

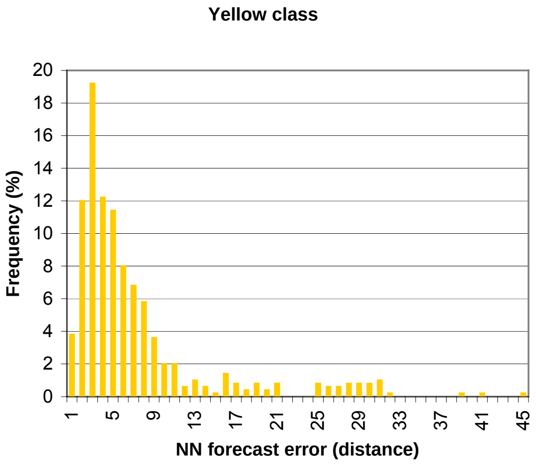

Figure 6. Error distribution in NN forecasts for the yellow class on the unforced attractor.

5. AN OPERATIONAL ESTIMATION OF PREDICTABILITY

In the previous section, the sensitivity of the forecasting performance of a NN model to different regions of predictability on Lorenz attractors has been shown. In this framework, peculiar increases in predictability and NN performance have been recognized when a weak external forcing is superimposed to the classical Lorenz system.

Even if some details of NN modeling must be better considered (I will briefly deal with them in the concluding section), this approach reveals a concrete application of an artificial intelligence technique to the analysis of predictability in a toy system which shows important meteo-climatic features.

Nevertheless, the consideration of NN forecasting performance represents just an *a posteriori* recognition of the predictability of the initial state on the Lorenz attractors. In fact it is available only after our knowledge of the results of the dynamical integration of the Lorenz system, while, from an operational point of view, the single NN forecasts give us just information about a possible trajectory, with no relation to predictability.

Thus, we could search for methods which can lead NN modeling to achieve an estimation of predictability on the Lorenz attractors which is fully operational. In this framework, in a previous paper (Pasini and Pelino 2005) the increase in the amplitude of error bars in NN performance when going from low bred-growth rates to high ones has been recognized. This led to explore a NN ensemble forecast approach by supposing that the spread of NN ensemble forecasts on distinct points could resemble a similar increase and could become an index of the peculiar local predictability of any Lorenz state. Unfortunately, the not very good NN forecasting performance (to be briefly discussed later) did not permit to find significant results by this attempt.

In this paper I will follow a different approach: a NN forecast of bred-growth rates for any point of the attractors is performed, leading us to obtain a direct estimation of this variable, which well represents the local predictability values. In doing so, NNs endowed with 3 inputs, one hidden layer (in which the number of neurons is more than doubled) and 1 output are used.

As shown in Table 5, even if the networks adopted here are very simple, the NN forecasts of bred-growth rate show quite good performance and contribute to open a new scenario in which NNs could be operationally used for estimations of the local predictability referred to single states on the Lorenz attractors. Furthermore, a statistical significant increase in performance is shown when an external forcing is applied. This result reveals that, not only the presence of an external forcing permits to better forecast the future states on the attractors (as shown in the previous section), but also the NN estimation of the predictability itself is improved in these forced situations.

	$f_0 = 0$	$f_0 = 5$
R	0.660 ± 0.011	0.684 ± 0.010

Table 5. Performance of NN estimation of the bred-growth rates on the test sets in terms of the linear correlation coefficient (NN forecasts vs. calculated values through dynamical integration). The error bars represent $\pm$ 2 standard deviations.

In order to obtain some more piece of information on the ability of the NN model to recognize different classes of predictability, I perform a simple statistical analysis by means of a contingency table (Table 6), where the threshold for bred-growth rate is fixed to 0.04: this value allows us to understand how well NNs can discern about situations in which trajectories may be undergone to "bifurcations" or not (see the discussions above).

DET \ FOR	No	Yes	Sum
No	*a*	*b*	*g*
Yes	*c*	*d*	*h*
Sum	*e*	*f*	*n*

Table 6. Contingency table at a defined threshold distinguishing between events and nonevents.

Referring to Table 6, several indices of performance are calculated as follows for two runs of the NN model:

POD (Probability Of Detection) = $d\,/\,h$;
FAR (False Alarm Ratio) = $b\,/\,f$;
HR (Hit Rate) = $(a+d)/\,n$;
CSI (Critical Success Index) = $d\,/(b+h)$;
HSS (Heidke's Skill Statistics) = $[2(ad-bc)]/(gf+he)$.

The results are shown in Table 7. As one can see, the forecasting performance in estimating local predictability is always better in the forced situation. Because of the goodness of HSS as a measure of performance (see, for instance, the discussion in Marzban 1998) the big difference in its values appears as particularly significant.

Index	$f_0 = 0$	$f_0 = 5$
POD	0.907	0.941
FAR	0.154	0.138
HR	0.810	0.841
CSI	0.778	0.818
HSS	0.289	0.512

Table 7. Indices of performance in NN forecasts of the bred-growth rate (threshold = 0.04).

Even if the performance results are not very good in absolute terms, however this section has shown that NNs are able to estimate local predictability on the Lorenz attractors and that this estimation is more performant in a forced situation, when compared with an unforced one.

6. CONCLUSIONS AND PROSPECTS

In this paper I have applied a non-dynamical approach (NN modeling) to the analysis of predictability in unforced and forced Lorenz systems.

A first result obtained here is that the performance of NNs in forecasting future states on the Lorenz attractors depends on the predictability class of the states themselves. In this framework, when passing from the unforced Lorenz system to a forced one, predictability increases and, analogously, NN performance increases as well. This preliminary result shows the sensitivity of NN forecasting to the values of local predictability and leads to rediscover an increase of predictability in forced situations also by a non-dynamical method. However, it does not permit to obtain an operational estimation of the predictability itself.

In section 5, this operational estimation has been achieved by directly forecasting the values of bred-growth rate through NNs. In this context, we have seen that the presence of a weak external forcing leads to better forecasting the future states of the system (as shown in section 4). Even more significative is the recognition that local predictability is operationally better forecasted in a forced situation.

Therefore, by exploring the simple case studies related to unforced and forced Lorenz systems (here considered as toy models of the climate and its atmospheric subsystem), the present paper leads to envisage an increased predictability in future meteo-climatic scenarios characterized by increased anthropogenic external forcings.

Of course, this paper reveals the need of improving the treatment of some critical points and opens perspectives of further work, too. For example, as cited above, the NN performance is not very good in the results described in sections 4 and 5. This can be due to the limited length of the record containing input-target pairs for training and validation, to the very preliminary structure of the input patterns themselves and to the simple architecture and training rules of the NNs used in this study.

Thus, possible developments of this work concern the building of an extended data set by prolonged Runge-Kutta integrations, the insertion of different inputs (for instance a truncated time series of delayed data) and the application of other NN architectures (such as recurrent NNs) and training rules.

In short, even if the present paper represents a quite preliminary attempt at exploring the role of NN modeling in studies about predictability, it shows that a new road for assessing and forecasting predictability is possible in a simple dynamical system; I think that an application to more realistic and complex models may be envisaged as well.

ACKNOWLEDGEMENTS

I am grateful to M. Peña and E. Kalnay for having gently allowed me to use their code for the calculation of bred vectors.

REFERENCES

Annan, J.D., 2005: Parameter estimation using chaotic time series, *Tellus*, **57A**, 709-714.

Atiya, A.F., S.M. El-Shoura, S.I. Shaheen, and M.S. El-Sherif, 1999: A comparison between neural-network forecasting techniques - Case study: river flow forecasting, *IEEE Trans. Neural Networks,* **10**, 402-409.

Bishop, C.M., 1995: *Neural networks for pattern recognition*, Oxford University Press, 482 pp.

Boudjema, G., and B. Cazelles, 2001: Extraction of nonlinear dynamics from short and noisy time series, *Chaos, Solit. and Fract.*, **12**, 2051-2069.

Briggs, K., 1990: An improved method for estimating Lyapunov exponents of chaotic time series, *Phys. Lett.*, **A151**, 27-32.

Corti, S., F. Molteni, and T.N. Palmer, 1999: Signature of recent climate change in frequencies of natural atmospheric circulation regimes, *Nature*, **398**, 799-802.

de Oliveira, K.A., A. Vannucci, and E.C. da Silva, 2000: Using artificial neural networks to forecast chaotic time series, *Physica*, **A284**, 393-404.

Evans, E., N. Bhatti, J. Kinney, L. Pann, M. Peña, S.-C. Yang, E. Kalnay, and J. Hansen, 2004: RISE undergraduates find that regime changes in Lorenz's model are predictable, *Bull. Amer. Meteor. Soc.*, **85**, 520-524.

Hertz, J., A. Krogh, and R.G. Palmer, 1991: *Introduction to the theory of neural computation*, Addison-Wesley, 327 pp.

Khatiwala, S., B.E. Shaw, and M.A. Cane, 2001: Enhanced sensitivity of persistent events to weak forcing in dynamical and stochastic systems: implications for climate change, *Geophys. Res. Lett.*, **28**, 2633-2636.

Lorenz, E.N., 1963: Deterministic non-periodic flow, *J. Atmos. Sci.*, **20**, 130-141.

Marzban, C., 1998: Scalar measures of performance in rare-event situations, *Weather Forecasting*, **13**, 753-763.

Mittal, A.K., S. Dwivedi, and A.C. Pandey, 2005: Bifurcation analysis of a paradigmatic model of monsoon prediction, *Nonlin. Proc. Geophys.*, **12**, 707-715.

Palmer, T.N., 1993: A nonlinear dynamical perspective on climate change, *Weather*, **48**, 313-326.

Palmer, T.N., 1999: A nonlinear dynamical perspective on climate prediction, *J. Clim.*, **12**, 575-591.

Pasini, A., 2005: *From observations to simulations. A conceptual introduction to weather and climate modelling*, World Scientific, 201 pp.

Pasini, A., 2007: Neural network modeling in climate change studies, in *Artificial intelligence methods in the environmental sciences* (Haupt, S.E., C. Marzban, and A. Pasini eds.), Springer (in press).

Pasini, A., and F. Ameli, 2003: Radon short range forecasting through time series preprocessing and neural network modeling, *Geophys. Res. Lett.*, **30 (7)**, 1386, doi:10.1029/2002GL016726.

Pasini, A., F. Ameli, and M. Lorè, 2003a: Mixing height short range forecasting through neural network modeling applied to radon and meteorological data, *Proc. 83rd AMS annual meeting (Third Conference on artificial intelligence applications to the environmental science)*, Long Beach, CA, AMS, CD-ROM, paper 3.5.

Pasini, A., M. Lorè, and F. Ameli, 2006: Neural network modelling for the analysis of forcings/temperatures relationships at different scales in the climate system, *Ecol. Model.*, **191**, 58-67.

Pasini, A., and V. Pelino, 2000: A unified view of Kolmogorov and Lorenz systems, *Phys. Lett.*, **A275**, 435-446.

Pasini, A., and V. Pelino, 2005: Can we estimate atmospheric predictability by performance of neural network forecasting? The toy case studies of unforced and forced Lorenz models, *Proc. IEEE International Conference on computational intelligence for measurement systems and applications (CIMSA 2005)*, Giardini Naxos, Italy, IEEE, pp. 69-74.

Pasini, A., V. Pelino, and S. Potestà, 2001: A neural network model for visibility nowcasting from surface observations: Results and sensitivity to physical input variables, *J. Geophys. Res.*, **106 (D14)**, 14,951-14,959.

Pasini, A., C. Perrino, and A. Žujić, 2003b: Non-linear atmospheric stability indices by neural-network modelling, *Nuovo Cimento*, **26C**, 633-638.

Pasini, A., and S. Potestà, 1995: Short-range visibility forecast by means of neural-network modelling: a case study, *Nuovo Cimento*, **18C**, 505-516.

Roebber, P.J., and A.A. Tsonis, 2005: A method to improve prediction of atmospheric flow transitions, *J. Atmos. Sci.*, **62**, 3818-3824.

Takens F., 1981: Detecting strange attractors in turbulence, in *Dynamical systems and turbulence* (Rand, D.A., and L.-S. Young eds.), Lecture Notes in Mathematics, Vol. 898, Springer, pp. 366-381.

Wolf, A., J.B. Swift, H.L. Swinney, and J.A. Vastano, 1985: Determining Lyapunov exponents from a time series, *Physica*, **D16**, 285-317.

Yadav, R.S., S. Dwivedi, and A.K. Mittal, 2005: Prediction rules for regime changes and length in a new regime for the Lorenz model, *J. Atmos. Sci.*, **62**, 2316-2321.